jove

Use of Minimally Invasive Methods to Assess Fuel Utilization and Circadian Rhythms in Older Adults

Christian McLaren[1,2], **Carly Bohlman**[1], **Armin Ezzati**[1], **Karyn Esser**[1], **Christiaan Leeuwenburgh**[1], **Todd Manini**[3], **Marco Pahor**[1], **Stephen Anton**[1,2], **Stephanie E. Wohlgemuth**[1]

[1] Department of Physiology and Aging, University of Florida [2] Department of Clinical and Health Psychology, College of Public Health and Health Professions, University of Florida [3] Department of Health Outcomes and Bioinformatics, University of Florida

Corresponding Authors

Stephen Anton
santon@ufl.edu

Stephanie E. Wohlgemuth
steffiw@ufl.edu

Citation

McLaren, C., Bohlman, C., Ezzati, A., Esser, K., Leeuwenburgh, C., Manini, T., Pahor, M., Anton, S., Wohlgemuth, S.E. Use of Minimally Invasive Methods to Assess Fuel Utilization and Circadian Rhythms in Older Adults. *J. Vis. Exp.* (203), e64628, doi:10.3791/64628 (2024).

Date Published

January 5, 2024

DOI

10.3791/64628

URL

jove.com/video/64628

Abstract

Aging is associated with multiple physiological changes that contribute synergistically and independently to physical disability and the risk of chronic disease. Although the etiology of age-related physical disability is complex and multifactorial, the decline in mitochondrial function appears to coincide with the progression of functional decline in many older adults. The reason why there is a decrease in mitochondrial function with aging remains elusive, but emerging science indicates that both fuel metabolism and circadian rhythms can influence mitochondrial function.

Recent studies have established that circadian rhythms become disturbed with aging, and that disrupted circadian rhythms have pathological consequences that impact mitochondrial function and overlap with many age-associated chronic diseases. Current quantitative methods for direct assessment of mitochondrial function are invasive and typically require a muscle biopsy, which can pose difficulties with participant recruitment and study adherence, given the perceived levels of potential pain and risk. Thus, an innovative and relatively noninvasive protocol to assess changes in mitochondrial function at the cellular level and circadian patterns in older adults was adapted. Specifically, a real-time metabolic flux analyzer is used to assess the mitochondrial bioenergetic function of white blood cells under differential substrate availability.

The expression of circadian clock genes in white blood cells to cross-correlate with the mitochondrial bioenergetics and circadian rhythm outcomes are also analyzed. It is believed that these innovative methodological approaches will aid future clinical trials by providing minimally invasive methods for studying mitochondrial substrate preference and circadian rhythms in older adults.

Introduction

Advancements in the past century have led to an increase in life expectancy and the population of aging adults. Looking to the future, the percentage of adults aged 65 years and older is projected to increase by 5% from 2020 to 2050 in the United States[1]. This increase in life expectancy does not imply an increase in health span-the period of life associated with independent functioning. The reality is that aging is accompanied by countless biological changes that affect cellular metabolism and physiology, producing gradual declines in cognitive and physical functioning[2,3]. As human life expectancy continues to increase, there is a greater need to preserve functional ability and independence with age[4].

It has been long known that the decline in physical function and independence with age is multifactorial, though it is frequently associated with the onset of chronic disease and acute inciting events[5]. Conversely, it has been shown that these declines in physical performance and muscle characteristics are associated with the development of disability with age with no clear connection to a single disease[6]. With the difficulties in knowing the exact etiology of chronic disease and physical disability, impairments in mitochondrial function have been thought to coincide with the onset and progression of chronic disease and loss of physical function in aging adults[7,8].

The mitochondria provide the majority of adenosine triphosphate (ATP), necessary for many cellular processes[9]. Highly oxidative tissues rely on mitochondria for adequate energy production; with aging, oxidative capacity and mitochondrial ATP synthesis decline. This decline is due in part to oxidative damage to mitochondrial DNA (mtDNA), which results in an incremental accumulation of mtDNA mutations and deletions[10]. The accumulation of mtDNA mutations and deletions cause a decrease in the formation of functional electron transport chain proteins, thus causing a reduced ability of cells to produce ATP. The age-associated decline in mitochondrial function is most notable in highly oxidative tissues, such as the heart and skeletal muscle[11]. Studies have demonstrated that the gastrocnemius muscle mitochondria in older rat samples exhibit an approximately 50% reduction in ATP production and content compared to younger samples[12]. Furthermore, it has been shown that the capacity of mitochondrial ATP production in human skeletal muscle decreases by approximately 8% per decade of life[13]. These findings suggest that age-related declines in mitochondrial function may contribute to decreased energy production in organisms.

A key regulator of mitochondrial activity is thought to be peroxisome proliferator-activated receptor γ (PPARγ) coactivator-1 (PGC-1α)[14]. Deterioration in PGC-1α activity or a decline in its abundance leads to reduced mitochondrial oxidative activity, and consequently, impaired energy production. Furthermore, a decline in mitochondrial quality may affect skeletal muscle quality and subsequently lead to the development or exacerbation of sarcopenia, dynapenia, and functional capacity decline[15,16]. Evidence for the age-related concurrent decline in mitochondrial function and skeletal muscle quality suggests a connection between mitochondrial impairment and the pathogenesis of functional decline[17]. Recently, this has been confirmed in functional community-dwelling older adults, showing that reductions in skeletal muscle mitochondria metabolism predict mobility decline in this population[18]. Though the exact mechanism leading to mitochondrial decline with age

is unclear, recent evidence has highlighted a reciprocal interplay between the circadian clock and mitochondrial function, with consequences for mitochondrial fuel utilization and biogenesis[19].

Fuel utilization

Mitochondrial function appears to be influenced by fuel metabolism and the type of fuel utilized at the cellular level in skeletal muscle tissue[11]. During periods of fuel depletion, specifically carbohydrate depletion in humans, the fuel preference for (mitochondrial) energy production changes. At low glucose levels, the fuel preference shifts away from glucose to fatty acids and acid-derived ketone bodies. This metabolic switch is marked by the upregulation of lipid metabolism in adipocytes followed by an increased release of ketones into the blood[4]. The shift in fuel utilization from glucose to ketones with a ketogenic diet seems to have a beneficial effect on mitochondrial reactive oxygen species production, antioxidant defense, ATP synthesis, and biogenesis[20].

The metabolic switch from carbohydrate to lipid metabolism occurs in periods of low environmental nutrient availability and when glycogen stores have been depleted. When this switch is initiated, stored triglycerides are broken down into glycerol, a substrate for gluconeogenesis, and free fatty acids, which are transported to the liver to be oxidized *via* β-oxidation into acetyl coenzyme A (acetyl CoA). Ketone bodies are synthesized, mainly in the liver, by a two-step condensation of three acetyl CoA molecules to β-hydroxy-β-methylglutaryl-CoA, which are then further processed into ketone bodies, including acetoacetate and 3-βeta hydroxybutyrate[21]. These ketone bodies are distributed to tissues throughout the body, with the highest consumption occurring in the heart, brain, and skeletal muscle[21]. With aging, mitochondrial fatty acid oxidation becomes impaired, thus impacting the metabolic switch[22]. It has been proposed that impairments in mitochondrial fuel utilization lead to further mitochondrial dysfunction, which in turn contributes to age-related disease and functional decline[23].

Changes in mitochondrial oxygen consumption of peripheral blood mononuclear cells (PBMCs) have been studied to assess the patterns associated with dysfunction and vascularization. Hartman *et al.* conducted a study that aimed to determine the correlation between oxygen consumption and diversely mediated dilation, which was found to suggest a link between mitochondrial dysfunction and vascular smooth muscle cell dysfunction[24]. Concerning other organs, PBMCs have been correlated with higher cognitive and brain functioning, as determined by respirometry[25]. Thus, PBMC bioenergetics and respiration capacity can serve as potential biomarkers for assessing the functional capacity of organs or tissues throughout the body.

Circadian rhythm

Another important factor affecting mitochondrial health is circadian rhythm. Circadian rhythms are ~24 h oscillations in behavior and physiology that occur in the absence of environmental cues[26]. These rhythms function in a predictive way to support system and tissue homeostasis. The mechanism that underlies circadian rhythms is a transcription-translation feedback loop called the circadian clock[27]. It has been demonstrated over the last 15 years that the circadian clock mechanism exists in virtually all cells throughout the body[28]. In addition to keeping time, the molecular clock mechanism also contributes to a daily program of gene expression, referred to as circadian clock output[29]. The clock output genes are unique to each tissue type and are functionally associated with pathways important

for cell metabolism, autophagy, repair, and homeostasis. Recent evidence has shown that mitochondrial health is dependent on circadian clock function and influences mitochondrial function, including mitochondrial biogenesis, fuel utilization, and mitophagy[30].

Emerging evidence in both preclinical and clinical studies has demonstrated that throughout aging, there are disturbances in circadian rhythms[31]. These include disruptions in normal sleep and wake cycles, a diminished amplitude in core body temperature rhythms, and a delayed ability to adjust to shifts in phase[31]. One study, for example, challenged the circadian system of adult and old (20+ months) mice by shifting the light schedule by 6 h. It was found that the old mice took longer to re-entrain their activity patterns to the new light schedule[32]. Consistent with the changes in circadian behavior, analysis of the tissue clocks found that both central and peripheral tissue clocks were impaired in the aging cohort.

More recently, several groups have performed transcriptomic analysis of the circadian clock and clock output across different tissues with age[33]. The outcomes of these studies highlight that there is large-scale reprogramming of the circadian clock output with age. This means that even though the core clock maintains a timing function, the genes targeted for daily expression are largely different. For example, two studies have collected muscle biopsies from human subjects every 4 h for 24 h, the results determining that the peak and trough of clock gene expression are reversed between nocturnal rodents and diurnal humans[34,35,36]. This indicates that when clock gene expression is compared based solely on active versus rest phase (and not light vs. dark), the patterns of clock gene expression in the muscles are virtually the same between species. It is proposed that this age-associated change in clock output results in impairments in the regulation of pathways that include the known hallmarks of aging, such as mitochondrial function, DNA damage and repair, and autophagy[37].

Study rationale

The connection between mitochondrial function and decline in physical function is well established. However, the underlying cause of mitochondrial dysfunction remains a subject of debate. Recent research suggests that cellular fuel utilization and circadian rhythms may play a role in this process. Traditional methods for evaluating mitochondrial function, such as measuring mitochondrial oxygen consumption in a muscle biopsy sample, are often perceived as painful and invasive, which may discourage participation, particularly in populations with low muscle mass, such as frail and sarcopenic adults[38].

Given these limitations, there is a need for a less invasive method for assessing changes in cellular fuel utilization and circadian rhythm in older adults. This study aims to evaluate a novel, minimally invasive protocol that can be used to assess fuel metabolism and circadian rhythm in this population. The results of this study will contribute to a better understanding of age-related changes and the response to medical or behavioral interventions, serving as a model for future studies in this field.

Protocol

Procedures involving human participants have been approved by the research ethics committee (Florida Ethics Policy 1.0104) and the Institutional Review Board of the University of Florida.

1. Mitochondrial function

1. Isolation of peripheral blood mononuclear cells (PBMCs)

1. Collect PBMCs using special 8 mL blood collection tubes (16 mm x 125 mm; containing either 0.1 M sodium citrate anticoagulant or sodium heparin anticoagulant) (see **Table of Materials**).
   NOTE: The blood collection tubes contain blood separation media composed of a thixotropic polyester gel and a gradient medium (see **Table of Materials**) to enhance the separation of white blood cells.
2. Process the 8 mL cell preparation tubes within 2 h following collection to obtain viable results.
3. Mix the blood collection tubes after filling them with blood (either by gentle inversion or on a mixer) and keep at room temperature (RT) for a maximum of 2 h.
4. Centrifuge the blood collection tubes in a fitting swing-out rotor at 2,000 × *g* for 15 min (or equivalent to 30,000 G-min; do not exceed 2,000 × *g*) at RT.
   NOTE: These tubes are taller than a regular 15 mL centrifuge tube; therefore, additional attention must be paid to using the correct rotor.
5. Aspirate and discard into a biohazardous waste container ~80% of the plasma layer, and collect the cell layer from the blood collection tube (using a transfer pipet) in a 15 mL centrifuge tube.
   NOTE: When using a 15 mL tube, add 7 mL of cell layer and fill to 14 mL with sterile phosphate-buffered saline (PBS). The ratio of cells to PBS should be 1:1. Use multiple tubes if necessary. Mix gently by inverting.
6. Centrifuge in a swing-out rotor at 900 × *g* for 5 min (or equivalent to 4,500 G-min) at RT.
7. Without disturbing the cell pellet, aspirate the PBS solution and discard it into a biohazardous waste container.
8. Resuspend the cell pellet in 1 mL of basal medium (BM; see **Table of Materials**) by gently triturating. Add the BM to a total of 10 mL, and gently mix by inverting. Perform a cell count.
9. Centrifuge the cell suspension in a swing-out rotor at 900 × *g* for 5 min at RT.
   NOTE: When cells are used the same day for the bioenergetic assessment, proceed to step 1.1.10; if the cells are frozen for storage, proceed to step 1.1.13.
10. Calculate the volume of assay medium (AM; see **Table of Materials**) for resuspension of the next cell pellet to achieve the desired cell concentration.
    NOTE: For example, for a seeding density of 150,000 cells/well in 50 µL, the desired concentration of the cell suspension is 3 million cells/mL.
11. Without disturbing the cell pellet, aspirate the supernatant and discard it into a biohazardous waste container.
12. Resuspend the cell pellet gently in 1 mL or less of AM. Add AM to the total calculated volume for the desired cell concentration. The cells are now ready to be seeded into a coated cell culture plate (see **Table of Materials**).
    NOTE: The following steps are for freezing the cells for storage (1.1.13-1.1.16) and do not apply to the same-day procedure.

13. For freezing cells, aspirate the supernatant without disturbing the cell pellet and discard it into a biohazardous waste container.
14. Gently resuspend the cells in freezing media (see **Table of Materials**) at the desired concentration (5-10 million cells/mL). Aliquot desired volumes in labeled cryovials.
15. Slow-freeze the cell suspension using a freezing container (see **Table of Materials**) for a minimum of 4 h or overnight at -80 °C.
16. After 4 h, or the next morning, transfer the cryovials to liquid nitrogen storage, where they should reside in the vapor phase.
17. **The day before measurement**, coat the well bottoms of a cell culture microplate (see **Table of Materials**) with cell adhesive (see **Table of Materials**). Prepare the adhesive according to the manufacturer's instructions, with a recommended concentration of 22.4 µg/µL, by diluting the appropriate volume of adhesive stock solution in 0.1 M sodium bicarbonate (pH 8.0). Apply 25 µL of adhesive to each well of the cell culture microplate.
18. After 20 min, siphon off the remaining liquid from each well and wash the wells twice with 200 µL of sterile, purified water. Let the plate dry in the biosafety cabinet (for ~2 h).
19. Wrap the plate in aluminum foil or place it in a closed secondary container, and store it in a refrigerator at 4 °C.

2. Bioenergetic assessment of PBMCs with thereal-time metabolic flux analyzer

NOTE: Using a flux analyzer and the multi-mode reader (see **Table of Materials**), an optimal seeding density of 150,000 PBMCs per well, a final uncoupler carbonyl cyanide-4 (trifluoromethoxy) phenylhydrazone (FCCP) concentration of 2 µM, and a final Hoechst 33342 concentration of 4 µM (with an incubation time of at least 20 min post-injection) were determined.

1. To **hydrate sensor cartridges with hydrobooster**, remove the sensor cartridge with the utility plate from the box and place the cartridge "sensor up" on the bench. Pipet 200 µL of calibrant (see **Table of Materials**) into each well of the utility plate and place the hydrobooster firmly on the utility plate, followed by the sensor cartridge. Inspect and remove any trapped air bubbles, and place in a 37 °C non-CO_2 incubator overnight.
2. Turn on the flux analyzer and subsequently open the assay analysis software (see **Table of Materials**). Set the temperature to 37 °C. Leave the instrument on overnight to allow stabilization of the set temperature.

   NOTE: The following programming steps (1.2.4-1.2.10) can be done the day before or on the day of the experiment
3. To program the assay analysis software (see **Table of Materials**) file, open the **template** for the **Substrate Oxidation Stress Test**. Go to **Group Definitions**, open the **Injection Strategies** tab, edit the **Inhibitor + Sub Ox Stress Test** to **Etomoxir + Sub Ox Stress Test**, and add two more injection strategies: **UK5099 + Sub Ox Stress Test** and **BTPES + Sub Ox Stress Test**. Within each injection strategy, within the **Injection Condition** window, click on **A** for **Port A** and enter the

final concentration of the respective inhibitor (**Etomoxir: 4 µM; UK5099: 2 µM; BTPES: 3 µM**).

4. Click on **Ports B, C,** and **D**, and enter the respective final concentrations (**port B**: **oligomycin concentration** [**1.50 µM**], **port C**: **FCCP** [**2.0 µM**]; **port D**: **Rotenone + Antimycin A** [**0.5 µM**]). Add **Hoechst 33342**, **4 µM** to the **compounds** window for **port D**.

5. Open the **Pretreatments** tab and choose **pretreatments**, if applicable. For example: **Control**, **Experimental**, or **customary** (e.g., **Baseline** and **Follow up**). Add descriptions in the window underneath if needed.

6. Open the **Assay Media** tab and from the **Media** pull-down menu, choose **RPMI Medium, pH 7.4**, enter the **lot number**, **personnel preparing the media**, **time of preparation**, and the **supplements added to the media** (10 mM glucose, 2 mM glutamine, 1 mM pyruvate; see **Table of Materials**).

7. Open the **Cell Type** tab and enter **PBMC-Subject ID** as the **Name**, **PBMC** as the **Cell Type**, **150000** as the **Seeding density**, **Subject ID** as the **Source**, **personnel who prepared the cells**, **date of preparation**, and **day of cell thaw**, if applicable.

8. Click on **Generate Groups**, go to **Plate Map**, and assign the wells of the 96-well plate to the respective groups. Keep wells **A1**, **A12**, **H1**, and **H12** assigned as **background wells**.

9. Go to **Protocol**, check the **Equilibrate** box (default setting), and enter the following information: **Baseline**: five measurement cycles: 3 min mix, 0 min wait, and 3 min measure; **Media or Inhibitor (Port A)**: six measurement cycles: 3 min mix, 0 min wait, and 3 min measure; **Oligomycin (Port B)**: three measurement cycles: 3 min mix, 0 min wait, and 3 min measure; **FCCP (Port C)**: three measurement cycles: 3 min mix, 0 min wait, and 3 min measure; **Rotenone + Antimycin A + Hoechst 33342 (Port D)**: three measurement cycles: 3 min mix, 0 min wait, and 3 min measure.

10. On the day of the bioenergetic assessment, take the coated cell culture microplate from the refrigerator and allow it to warm up to RT in the biosafety cabinet.

11. Prepare assay medium (AM) by mixing 97 mL of prewarmed BM and supplements: 1 mL of pyruvate (final concentration: 1 mM), 1 mL of glucose (final concentration 10 mM), and 1 mL of glutamine (final concentration: 2 mM). Place the AM at 37 °C in a non-CO_2 incubator until use.

12. To seed the cells, add 50 µL of cell suspension (from 1.1.12) containing 150,000 PBMCs to each well, except **A1**, **H1**, **A12**, and **H12** (assigned as **background wells**).
    CRITICAL: The optimal seeding density has been determined previously.

13. Cover the cell plate with its lid and allow 60 min of cell rest at RT in the biosafety cabinet to facilitate the even distribution of cells.
    CRITICAL: View the cells under a microscope to ensure desired homogeneous cell distribution across the well.

14. For cell imaging, turn on the multi-mode reader (see the **Table of Materials**) a few hours before the first cell incubation; wait for the reader's initiation protocol to complete before opening the imaging software (see the **Table of Materials**).

Open the imaging software and set the **preheating temperature** to **37 °C**.

15. To prepare the assay reagents, follow the assay kit's instructions to reconstitute the reagents, with slight modifications as outlined in **Table 1**.
    CRITICAL: The optimal final FCCP and Hoechst33342 concentrations have been determined previously.

16. After the 60-minute cell rest, inspect the wells with a cell culture microscope and make note of any visual abnormalities, such as cell aggregations.

17. Centrifuge the cell culture plate at RT in a centrifuge with a swing-out rotor for microplates at 60 × *g* for 1 min, with minimum acceleration and minimum break; turn the plate and centrifuge again at 40 × *g* for 1 min. Set the acceleration and break to a minimum. Incubate the cells for 25-30 min at 37 °C in a non-CO_2 incubator.
    NOTE: When cell imaging is performed, the cell plate is incubated in the preheated multi-mode reader instead (see the **Table of Materials**), and a brightfield image is taken of each well during this incubation period (first cell incubation).

18. Scan the cell culture plate's barcode with the barcode scanner (see **Table of Materials**), select **Start Brightfield Scan**, place the cell culture plate on the plate tray, and initiate tray retraction. Select cells-containing wells for scanning and start the scan.

19. During the first cell incubation, **load the ports of the sensor cartridge** with the reagents, as indicated in **Table 1: port (A)**: 20 µL of AM (controls), etomoxir (inhibitor of long-chain fatty acid transport into the mitochondria), UK 5099 (2-Cyano-3-(1-phenyl-1H-indol-3-yl)-2-propenoic acid; inhibitor of mitochondrial pyruvate carrier), or BPTES (Bis-2-(5-phenylacetamido-1,3,4-thiadiazol-2-yl)ethyl sulfide; inhibitor of glutamine conversion to glutamate); **port (B)**: 22 µL of oligomycin (inhibitor of ATP synthase); **port (C)**: 25 µL of FCCP (uncoupler carbonyl cyanide-4 (trifluoromethoxy) phenylhydrazone); **port (D)**: 27 µL of rotenone/antimycin A/Hoechst 33342 (inhibitors of mitochondrial complex I and III, respectively, and nuclear dye). Return the sensor cartridge to the 37 °C non-CO_2 incubator for another 5 min.
    NOTE: Follow the manufacturer's instructions for port loading.

20. Take the cell culture plate out of the incubator or plate reader after the first cell incubation and after the cell imaging is completed (if applicable), and add warm AM to each well to a final volume of 180 µL per well. Place the cell plate at 37 °C in a non-CO_2 incubator for another 15-25 min (second cell incubation).

21. Initiate the **metabolic assay** by starting the sensor calibration during the second cell incubation. Click on **Run Assay** when the assay is ready to be started with the calibration of the sensor cartridge. When prompted, transfer the sensor cartridge from the 37 °C non-CO_2 incubator to the flux analyzer tray and start the calibration. Follow the assay analysis software prompt and replace the utility plate for the cell plate after calibration is completed.
    NOTE: Calibration takes approximately 20 min.

22. After the metabolic assay, follow the software prompt and remove the sensor cartridge and cell

plate from the instrument. Remove the sensor cartridge from the cell plate and cover the cell plate with its lid.

23. After the Hoechst dye incubation time has been determined in preliminary experiments, scan the plate's barcode and follow the software prompts to acquire a fluorescent image of each cell-containing well with the multi-mode reader.
    NOTE: The imaging and assay analysis software is interfaced, allowing for import of the cell count data into the assay analysis data file for data normalization to the cell count.

2. Circadian clock gene expression

NOTE: Participants' expression of clock genes from PBMCs will be reviewed by isolating RNA using the RNA blood kit (see **Table of Materials**).

1. Draw 3 mL of the participant's blood directly into a RNA tube (see **Table of Materials**) with 6 mL of stabilizing reagents. Vortex for 10 s to fully mix.
   NOTE: If stabilizing reagents are not thoroughly mixed with the participant's blood sample, then there is an increased risk of study error.
2. Transfer 1.0 mL of the stabilized blood sample to a 15 mL tube, with 5 mL of erythrocyte lysis buffer. Incubate on ice for 10-15 min. Vortex the tube 2x during the incubation. Centrifuge the tube at 4 °C at 400 × *g* for 10 min.
3. Identify the pellet and carefully pour off the supernatant containing lysed red blood cells. Add 2 mL of erythrocyte lysis buffer (see **Table of Materials**), resuspend the cells, vortex briefly, and centrifuge at 400 × *g* for 10 min at 4 °C.
4. Pour off the supernatant and leave the tube inverted on absorbent paper for 1-2 min. Blot off any liquid around the rim of the tube with clean paper before the next step.
5. Carefully add 600 µL of RNA lysis buffer (see **Table of Materials**). Following the manufacturer's protocol, add β-mercaptoethanol and resuspend the pellet.
6. Pipet the lysate directly into a disposable cell-lysate homogenizer (see **Table of Materials**) spin column placed in a 2 mL collection tube and centrifuge for 2 min at maximum speed to homogenize. Discard the disposable cell-lysate homogenizer spin column and save the homogenized lysate.
7. Add 1 volume (600 µL) of 70% ethanol to the homogenized lysate and mix by pipetting. Carefully pipet the sample, including any precipitate which may have formed, into a new spin column in a 2 mL collection tube, but do not moisten the rim. Centrifuge for 15 s at >8,000 × *g*.
8. Transfer the spin column (see **Table of Materials**) into a new 2 mL collection tube. Apply 700 µL of stringent washing buffer (see **Table of Materials**) to the spin column and centrifuge for 15 s at >8,000 × *g* to wash. Discard the flowthrough.
9. Carefully open the spin column and add 500 µL of mild washing buffer (see **Table of Materials**). Close the cap and centrifuge at full speed (20,000 × *g*) for 3 min.
10. Transfer the spin column into a 1.5 mL microcentrifuge tube and pipet 30-50 µL of RNase-free water directly onto the silica membrane. Centrifuge for 1 min at >8,000 × *g* to elute the RNA. Repeat once more.
    NOTE: The RNA can be stored at -80 °C.

11. Perform DNase treatment on a column using the RNase-free DNase set (see **Table of Materials**), according to the manufacturer's protocol.
12. Generate cDNA using 500 ng of total RNA and a real-time polymerase chain reaction (PCR) system (see **Table of Materials**), according to the manufacturer's protocol. Dilute all cDNA samples 1:25 in RNase-free water and use 4 mL to perform quantitative reverse transcription PCR (qRT-PCR).
13. Use a primer addition method (see **Table of Materials**) to complete qRT-PCR with 10 mM of each of the primers shown in Table 2. Complete qRT-PCR using a real-time system (see **Table of Materials**).
14. Normalize the mRNA levels of the chosen genes using *Rpl26* mRNA levels. Use the 2^{-DDCt} method to calculate the relative quantification.
15. To determine if the expression of a given mRNA exhibited a circadian oscillation, utilize an LR_rhythmicity[39] likelihood-based test (using $p \leq 0.01$) for detecting circadian rhythmicity in one experimental condition[40].

3. Data analysis plan

NOTE: A medical inventory will be used to categorize participants based on medication usage[43].

1. Use a mixed-effects linear model, in which age, gender, weight, height, blood pressure, heart rate, and other risk factors should be included as covariates.
2. A random-effect term should be included to explain the within-subject data correlation.
3. For model fitting, a backward variable selection with the hierarchical principle should be implemented.
4. From the fitted model, measure changes from timepoint 1 to timepoint 2, given all the covariates in the fitted model.

Representative Results

The proposed protocol includes preliminary data that serves as validation for the methodology. The protocol incorporates a real-time metabolic flux analyzer to examine mitochondrial function and cellular fuel utilization, and RNA extraction and qRT-PCR to analyze circadian rhythm genes (e.g., BMAL1, CLOCK, Nfil2, Nr1d1, Dbp, Cry1, Per2).

The oxygen consumption rate (OCR) of isolated human PBMCs from five control participants, 10 days after an initial analysis, is presented in **Figure 1**. The data is used to compare pre- and post-values and shows the average values for basal respiration, acute response, maximal respiration, and spare capacity following the injection of a control, etomoxir, UK5099, and BPTES. Notably, **Figure 1C** shows a significant negative acute response following the etomoxir injection, but no significant effects were observed for basal respiration, maximal respiration, or spare capacity.

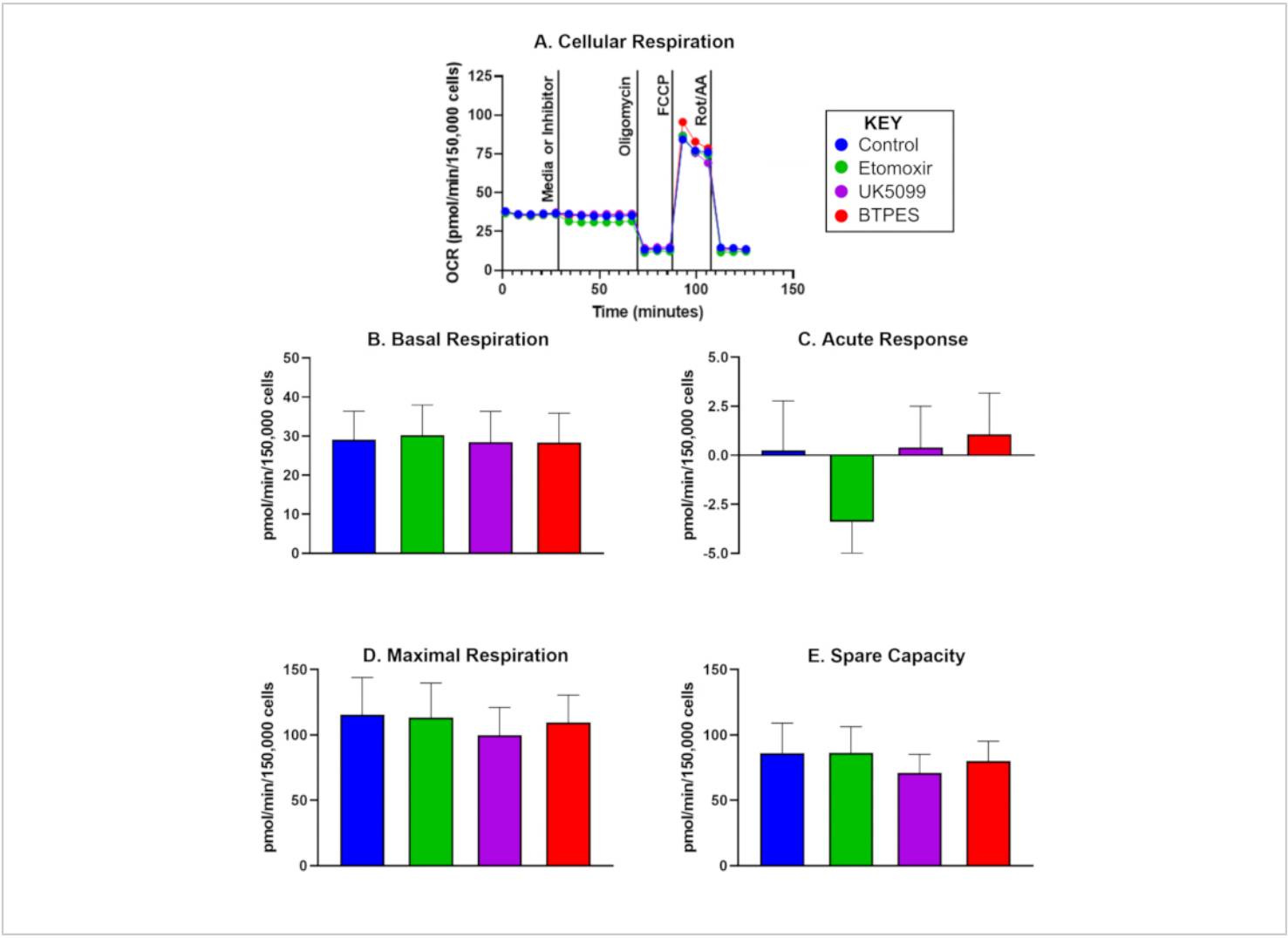

Figure 1: Oxygen consumption of isolated human peripheral blood mononuclear cells (PBMCs). (**A**) Real-time oxygen consumption rate (OCR; pmol/(min·150,000 cells) of PBMCs isolated from a control subject, measured with a Flux Analyzer and assessed with the substrate oxidation assay. Cells were seeded at a density of 150,000 cells/well. The first injection was either media (control) or inhibitor (etomoxir, UK5099, or BPTES; see text for details) and occurred after measuring the basal cellular respiration rate. The acute response to the mitochondrial substrate limitation was determined as the difference of basal OCR before and after inhibitor injection. Oligomycin, the ATP synthase inhibitor, inhibits ATP-production coupled respiration and yields proton leak respiration. FCCP, the uncoupler, induces maximal, uncoupled respiration; rotenone and antimycin A (inhibitors of complex I and III, respectively) inhibit all but non-mitochondrial respiration (see text for details). (**B-E**) Quantification of cellular respiration (n = 5; data are represented as mean ± SD). (**B**) Basal OCR before inhibitor injection, (**C**) acute response to the inhibitor (change in OCR relative to the basal rate before inhibitor injection), (**D**) maximal OCR, and (**E**) spare capacity (difference between maximal OCR and basal OCR after the first injection). The acute response (**C**) to etomoxir injection might suggest a higher dependence of OCR on fatty acid as an energy substrate under basal

conditions compared to the other substrate groups, without a noticeable effect on OCR during high energy demand (**D**).

Please click here to view a larger version of this figure.

Compound	AM (µL) added to compound	Stock (µM)	stock (µL) for working stock	AM (µL) for working stock	Working stock (µM)	Working stock (µL) [port]	Final conc. (µM)
Etomoxir	700	160	500	1500	40	20 [A]	4
UK5099	700	80	500	1500	20	20 [A]	2
BPTES	700	120	500	1500	30	20 [A]	3
oligo	420	150	300	2700	15	22 [B]	1.5
FCCP	720	100	600	2400	20	25 [C]	2
Rot/AA/H	540	50	300	2700	5	27 [D]	0.5

Table 1: Preparation of reagents for the substrate oxidation test and concentrations of stock, working, and final solutions. All reagents are part of the cell mito stress test or the substrate oxidation stress test kits. Abbreviations: oligo = oligomycin; FCCP = uncoupler carbonyl cyanide-4 (trifluoromethoxy) phenylhydrazone; Rot/AA/H = rotenone/antimycin A/ Hoechst 33342. Etomoxir, UK5099, BTPES: inhibitors of fatty acid, glucose, and glutamine oxidation, respectively.

Bmal1	**Forward** – GCACGACGTTCTTTCTTCTGT
	Reverse – GCAGAAGCTTTTTCGATCTGCTTTT
Clock	**Forward** – CGTCTCAGACCCTTCCTCAAC
	Reverse – GTAAATGCTGCCTGGGTGGA
Cry1	**Forward** – ACTGCTATTGCCCTGTTGGT
	Reverse – GACAGGCAAATAACGCCTGA
Per1	**Forward** – ATTCGGGTTACGAAGCTCCC
	Reverse – GGCAGCCCTTTCATCCACAT
Per2	**Forward** – CATGTGCAGTGGAGCAGATTC
	Reverse – GGGGTGGTAGCGGATTTCAT
Rev-erb α	**Forward** – ACAGATGTCAGCAATGTCGC
	Reverse – CGACCAAACCGAACAGCATC

Table 2: Circadian clock gene primers.

Discussion

The decline in mitochondrial function and regulation of circadian rhythm with age are increasingly viewed as contributing factors to age-related diseases. Altering circadian rhythms through lifestyle modifications, such as diet and physical activity, represents a potential strategy to promote healthy aging and reduce mobility declines associated with aging. However, current methods for directly evaluating mitochondrial function are invasive and often require a muscle biopsy, which can pose challenges with participant recruitment and retention due to perceived pain and risks.

Assessing markers of circadian and metabolic health through less invasive methods, such as blood collection, would provide valuable outcomes for exploring and testing therapeutic targets in future studies. These minimally invasive methods have the potential to greatly advance the field by providing new insights into the complex interplay between circadian rhythm and metabolic health and their impact on function. The goal of this study is to evaluate the relationship between cellular energy metabolism and circadian rhythm. In particular, bioenergetic flux analysis is used to evaluate mitochondrial function under various substrate availability conditions, along with gene expression monitoring of a group of circadian genes in participants' white blood cells. By employing both arms of the analysis, bioenergetic and gene expression, a comprehensive understanding of the relationship between these two fundamental processes can be achieved.

The statistical analysis of this time series data from a circadian perspective offers insight into the strength, range, and timing of the circadian rhythms. In conclusion, the integration

of gene expression analysis, cellular bioenergetics, and metabolic measures at the organism level constitutes a new and innovative approach that will shed light on the interplay between energy metabolism and circadian rhythms in humans.

In a pilot study, we detected an acute response in the OCR of PBMCs to the limitation of fatty acid utilization (following injection of etomoxir, an inhibitor of carnitine palmitoyl transferase 1a). This finding suggests that in PBMCs from this particular group of participants, there might be a dependence on fatty acids as an energy substrate during basal respiration. However, maximal respiration was not impacted, suggesting that alternative energy sources, such as glucose and glutamine, may compensate for the reduced utilization of fatty acids during high energy demand. Future studies should investigate whether a) bioenergetics of PBMCs are reflective of whole-body energetics and b) whether interventions such as time restricted eating could affect energy substrate preferences.

There are several critical steps concerning the flux analysis of PBMCs. First, before experimental samples are assessed, the cell seeding density (cells per well) should be optimized by making sure that there is a continuous uniform distribution of cells within each well and across each plate, the final FCCP concentration should be optimized by running concentrations test runs using the concentrations 0, 0.125, 0.25, 0.5, 1.0, and 2.0 µM, and, if applicable, the Hoechst 33342 staining should be optimized by following the manufacturer's instructions. Second, the normalization of the metabolic data to cellular parameters is critical for the comparability of the data between experiments. In the present protocol, cell count after the conclusion of the flux analyzer assay using Hoechst 33342-stained cells and a cell imaging device is described. If an appropriate device is not available, alternative normalization methods can be applied, such as total cellular protein or nuclear DNA content per well. There is a noted modification that can be utilized within the protocol, compared to those that have been proposed. Specifically, the protocol can be completed utilizing an individual assay kit for each of the three inhibitors, compared to just the two kits proposed here (see **Table of Materials**).

The use of PBMCs as a surrogate to study the interplay between energy metabolism and circadian rhythms in older adults is limited by the assumption that their response to treatment can accurately reflect the response in other tissues and organs. Although this approach is novel and minimally invasive, it is important to acknowledge that different tissues and organs, such as the brain, liver, and skeletal muscle, may react differently under various conditions. A preclinical study demonstrated that clock gene expression was altered in fed and fasted mice, leading to the partial upregulation of BMAL1-target genes in liver and muscle tissue, but the downregulation of others[41]. These peripheral tissues and organs are highly representative of metabolic processes and can be influenced by environmental cues that impact clock gene expression mechanisms[42]. Further research is needed to fully understand the relationship between peripheral tissues, organs, and the central circadian clock.

Another limitation is that participants are not disqualified for taking any prescription, which might pose limitations to statistical analysis. To counteract this limitation, in future research, a medical inventory will be used, which has been validated in populations of older adults who take medications[43]. Participants will be categorized based on the recommended medications recorded in the protocol's data review section. There are a total of three categories, in

terms of medications that have been shown to 1) accelerate functional decline, 2) slow functional decline, and 3) influence skeletal muscle function.

Lastly, human skeletal muscle mitochondrial oxidative capacity does exhibit a day-night rhythm, peaking between 06:00 pm and 11:00 pm and declining between 08:00 am and 11:00 am[44]. It is not yet clear if this holds for the mitochondrial oxidative capability of PBMCs. However, preliminary data suggest that PBMCs and mitochondrial metabolism are related[45]. Given that the information on muscle biopsies and the alterations in PBMCs is not as clear, caution must be taken when analyzing results. Given this limitation, it is important to keep this information in mind when evaluating and developing a protocol, as it may provide valuable context and insight that could aid in ensuring the validity and effectiveness of the protocol.

To the best of our knowledge, no prior studies have assessed the patterns of fuel utilization or circadian rhythms through the methods proposed in this project. Our objective is to examine the responsiveness of markers of mitochondrial fuel utilization and circadian health to changes. This study presents a minimally invasive method for measuring a highly sensitive biomarker, which can serve as an alternative in future interventional studies where muscle biopsy is not feasible.

Disclosures

The authors have no conflicts of interest to disclose.

Acknowledgments

This study was funded by the Older American's Independence Center (NIH/NIA P30AG028740), with assistance from the Clinical and Translational Science Institute (NIH/NCRR UL1TR000064).

References

1. UN Department of Economic and Social Affairs. Population Division 2019, *World Population Prospects.* (2019).
2. Anton, S., Leeuwenburgh, C. Fasting or caloric restriction for healthy aging. *Experimental Gerontology.* **48** (10), 1003-1005 (2013).
3. Dziechciaż, M., Filip, R. Biological psychological and social determinants of old age: Bio-psycho-social aspects of human aging. *Annals of Agricultural and Environmental Medicine.* **21** (4), 835-838 (2014).
4. Anton, S. D. et al. Flipping the metabolic switch: understanding and applying the health benefits of fasting. *Obesity.* **26** (2), 254-268 (2018).
5. Fried, L. P., Guralnik, J. M. Disability in older adults: evidence regarding significance, etiology, and risk. *Journal of the American Geriatrics Society.* **45** (1), 92-100 (1997).
6. Manini, T. Development of physical disability in older adults. *Current Aging Science.* **4** (3), 184-191 (2011).
7. Chung, H. Y. et al. Molecular inflammation: underpinnings of aging and age-related diseases. *Ageing Research Reviews.* **8** (1), 18-30 (2009).
8. Sun, N., Youle, R. J., Finkel, T. The mitochondrial basis of aging. *Molecular Cell.* **61** (5), 654-666 (2016).
9. Tarasov, A. I., Griffiths, E. J., Rutter, G. A. Regulation of ATP production by mitochondrial Ca^{2+}. *Cell Calcium.* **52** (1), 28-35 (2012).

10. Chistiakov, D. A., Sobenin, I. A., Revin, V. V., Orekhov, A. N., Bobryshev, Y. V. Mitochondrial aging and age-related dysfunction of mitochondria. *Biomed Research International.* **2014**, 238463 (2014).

11. Boengler, K., Kosiol, M., Mayr, M., Schulz, R., Rohrbach, S. Mitochondria and ageing: role in heart, skeletal muscle and adipose tissue. *Journal of Cachexia, Sarcopenia, and Muscle.* **8** (3), 349-369 (2017).

12. Drew, B. et al. Effects of aging and caloric restriction on mitochondrial energy production in gastrocnemius muscle and heart. *American Journal of Physiology Regulatory, Integrative and Comparative Physiology.* **284** (2), R474-R480 (2003).

13. Short, K. R. et al. Decline in skeletal muscle mitochondrial function with aging in humans. *Proceedings of the National Academy of Sciences.* **102** (15), 5618-5623 (2005).

14. Musci, R. V., Hamilton, K. L., Miller, B. F. Targeting mitochondrial function and proteostasis to mitigate dynapenia. *European Journal of Applied Physiology.* **118** (1), 1-9 (2018).

15. Picca, A. et al. Targeting mitochondrial quality control for treating sarcopenia: lessons from physical exercise. *Expert Opinion on Therapeutic Targets.* **23** (2), 153-160 (2019).

16. Fernandez-Marcos, P. J., Auwerx, J. Regulation of PGC-1α, a nodal regulator of mitochondrial biogenesis. *The American Journal of Clinical Nutrition.* **93** (4), 884S-890 (2011).

17. Kim, Y., Triolo, M., Hood, D. A. Impact of aging and exercise on mitochondrial quality control in skeletal muscle. *Oxidative Medicine and Cellular Longevity.* **2017**, 3165396 (2017).

18. Wang, H., Hiatt, W. R., Barstow, T. J., Brass, E. P. Relationships between muscle mitochondrial DNA content, mitochondrial enzyme activity and oxidative capacity in man: alterations with disease. *European Journal of Applied Physiology and Occupational Physiology.* **80** (1), 22-27 (1999).

19. Tian, Q. et al. Muscle mitochondrial energetics predicts mobility decline in well-functioning older adults: The baltimore longitudinal study of aging. *Aging Cell.* **21** (2), e13552 (2022).

20. Sardon Puig, L., Valera-Alberni, M., Cantó, C., Pillon, N. J. Circadian rhythms and mitochondria: connecting the dots. *Frontiers in Genetics.* **9**, 452 (2018).

21. Gano, L. B., Patel, M., Rho, J. M. Ketogenic diets, mitochondria, and neurological diseases. *Journal of Lipid Research.* **55** (11), 2211-2228 (2014).

22. Liesa, M., Shirihai, O. S. Mitochondrial dynamics in the regulation of nutrient utilization and energy expenditure. *Cell Metabolism.* **17** (4), 491-506 (2013).

23. Lesnefsky, E. J., Chen, Q., Hoppel, C. L. Mitochondrial metabolism in aging heart. *Circulation Research.* **118** (10), 1593-1611 (2016).

24. Hartman, M. L. et al. Relation of mitochondrial oxygen consumption in peripheral blood mononuclear cells to vascular function in type 2 diabetes mellitus. *Vascular Medicine.* **19** (1), 67-74 (2014).

25. Mahapatra, G. et al. Blood-based bioenergetic profiling is related to differences in brain morphology in African Americans with Type 2 diabetes. *Clinical Science.* **132** (23), 2509-2518 (2018).

26. Moore-Ede, M. C. Physiology of the circadian timing system: predictive versus reactive homeostasis. *The American Journal of Physiology.* **250** (5 Pt 2), R737-R752 (1986).

27. Young, M. W. Life's 24-hour clock: molecular control of circadian rhythms in animal cells. *Trends in Biochemical Sciences.* **25** (12), 601-606 (2000).

28. Yoo, S. H. et al. PERIOD2::LUCIFERASE real-time reporting of circadian dynamics reveals persistent circadian oscillations in mouse peripheral tissues. *Proceedings of the National Academy of Sciences.* **101** (15), 5339-5346 (2004).

29. Zhang, R., Lahens, N. F., Ballance, H. I., Hughes, M. E., Hogenesch, J. B. A circadian gene expression atlas in mammals: implications for biology and medicine. *Proceedings of the National Academy of Sciences.* **111** (45), 16219-16224 (2014).

30. de Goede, P., Wefers, J., Brombacher, E. C., Schrauwen, P., Kalsbeek, A. Circadian rhythms in mitochondrial respiration. *Journal of Molecular Endocrinology.* **60** (3), R115-R130 (2018).

31. Hood, S., Amir, S. The aging clock: circadian rhythms and later life. *The Journal of Clinical Investigation.* **127** (2), 437-446 (2017).

32. Sellix, M. T. et al. Aging differentially affects the re-entrainment response of central and peripheral circadian oscillators. *The Journal of Neuroscience.* **32** (46), 16193-16202 (2012).

33. Sato, S. et al. Circadian reprogramming in the liver identifies metabolic pathways of aging. *Cell.* **170** (4), 664-677.e11 (2017).

34. Lundell, L. S. et al. Time-restricted feeding alters lipid and amino acid metabolite rhythmicity without perturbing clock gene expression. *Nature Communications.* **11** (1), 4643 (2020).

35. Perrin, L. et al. Transcriptomic analyses reveal rhythmic and CLOCK-driven pathways in human skeletal muscle. *eLife.* **7**, e34114 (2018).

36. Gutierrez-Monreal, M. A., Harmsen, J.-F., Schrauwen, P., Esser, K. A. Ticking for metabolic health: the skeletal-muscle clocks. *Obesity.* **28** (Suppl 1), S46-S54 (2020).

37. Wolff, C. A. et al. Defining the age-dependent and tissue-specific circadian transcriptome in male mice. *bioRxiv.* **42** (1), 111982 (2023).

38. Wilson, D., Breen, L., Lord, J. M., Sapey, E. The challenges of muscle biopsy in a community based geriatric population. *BMC Research Notes.* **11** (1), 830 (2018).

39. Ding, H. et al. Likelihood-based tests for detecting circadian rhythmicity and differential circadian patterns in transcriptomic applications. *Briefings in Bioinformatics.* **22** (6), bbab224 (2021).

40. Ding, Z., Lamb, T. M., Boukhris, A., Porter, R., Bell-Pedersen, D. Circadian clock control of translation initiation factor eIF2α activity requires eIF2γ-dependent recruitment of rhythmic PPP-1 phosphatase in Neurospora crassa. *mBio.* **12** (3), e00871-21 (2021).

41. Di Francesco, A., Di Germanio, C., Bernier, M., de Cabo, R. A time to fast.*Science.* **362** (6416), 770-775 (2018).

42. Kalfalah, F. et al. Crosstalk of clock gene expression and autophagy in aging. *Aging.* **8** (9), 1876-1895 (2016).

43. Psaty, B. M. et al. Assessing the use of medications in the elderly: methods and initial experience in

the cardiovascular health study. *Journal of Clinical Epidemiology.* **45** (6), 683-692 (1992).

44. van Moorsel, D. et al. Demonstration of a day-night rhythm in human skeletal muscle oxidative capacity. *Molecular Metabolism.* **5** (8), 635-645 (2016).

45. Janssen, J. J. E. et al. Extracellular flux analyses reveal differences in mitochondrial PBMC metabolism between high-fit and low-fit females. *American Journal of Physiology. Endocrinology and Metabolism.* **322** (2), E141-E153 (2022).